INFLUENCE OF SILICON NITRIDE AND ITS HYDROGEN CONTENT ON CARRIER-INDUCED DEGRADATION IN MULTICRYSTALLINE SILICON

Carlos Vargas[1], Kyung Kim[1], Gianluca Coletti[1,2], David Payne[1], Catherine Chan[1], Stuart Wenham[1] and Ziv Hameiri[1]
[1] School of Photovoltaic and Renewable Energy Engineering, University of New South Wales, Sydney, Australia
[2] Energy Research Centre of the Netherlands, the Netherlands

ABSTRACT: Multicrystalline silicon (mc-Si) wafers show degradation due to carrier injection. This carrier-induced degradation particularly limits the performance of passivated emitter rear cell (PERC) made with mc-Si and is, therefore, gaining increasing attention from the photovoltaic community, as it is expected that PERC architecture will become dominant in the near future. In this study, we investigated the degradation behaviour of mc-Si wafers with six different silicon nitride passivation layers which were then separately fired at six different peak temperatures (a matrix of 36 conditions). We found that wafers fired at a low peak temperature (< 650 °C) had similar degradation rates independent of the silicon nitride deposition conditions, whilst the degradation rate of samples fired at higher temperature showed a clear dependence on these conditions. At high firing temperatures normally used for contact formation, it appears that there is a correlation between the degradation rate and the amount of hydrogen released from the dielectric during firing. Furthermore, we verified that no degradation of the surface passivation quality occurs, indicating that the degradation is primarily associated with a bulk-related defect.

Keywords: Multicrystalline silicon, Degradation, Silicon-Nitride, Hydrogen

1 INTRODUCTION

Light and elevated temperature induced degradation (LeTID) in multicrystalline silicon (mc-Si) wafers were first reported by Ramspeck *et al.* in 2012 [1]. Kersten *et al.* [2] found that this degradation can be induced by current injection and is faster under open-circuit than under short-circuit conditions; therefore, it is also known as carrier-induced degradation (CID) [2], [3]. The formation of a boron-oxygen (B-O) complex has been discarded as a possible cause: (i) as mc-Si doped with gallium (Ga) also presents CID [1], (ii) mc-Si is characterized by low interstitial oxygen (O_i) concentrations in comparison with Czochralski (Cz) silicon, and (iii) the time scales of CID formation defect and regeneration rates are much slower than those of B-O [2].

Fertig *et al.* [4] reported more pronounced degradation in mc-Si cells with an aluminium oxide (AlO_x) passivation layer than in full-area aluminium back surface field mc-Si cells. Therefore, they concluded that the AlO_x surface passivation could play a role in CID formation. Recently, Kersten *et al.* [5] reported different CID rates for mc-Si lifetime samples passivated with AlO_x, silicon nitride (SiN_x) and AlO_x/SiN_x stack layers. Particularly, they used two SiN_x layers deposited by two different industrial systems and reported differences in the degradation rates. This was the first indication that the SiN_x properties can influence CID rate. However, the deposition conditions and the SiN_x properties were not reported.

It is also known that CID has a strong dependence on the firing conditions [6], [7]. Higher peak firing temperatures lead to more pronounced degradation. CID is less severe in samples fired at low temperature (< 600 °C) and it is not present in non-fired samples [6].

In this study, we vary the deposition parameters to investigate their impact on the CID extent and its formation and regeneration rates.

2 EXPERIMENTAL METHOD

Neighbouring six inch conventional *p*-type mc-Si wafers with a thickness of ~ 190 µm and resistivity of 1.9 Ω.cm were used to fabricate symmetrical lifetime test structures. Processing included: RCA (Radio Corporation of America) cleaning followed by a light phosphorous diffusion (both sides; carried out in a Tempress $POCl_3$ tube) to form a doped layer with a sheet resistance of 80 Ω/□. Subsequently, the wafers received a hydrofluoric acid (HF) dip followed by a SiN_x deposition [8]. These test structures were divided into six different groups, where each group was symmetrically deposited with a SiN_x layer on both sides using a Meyer Burger MAiA plasma-enhanced chemical vapour deposition (PECVD) system (see Table I for the deposition conditions and properties of each layer). In parallel, six Cz double-side polished wafers were prepared using the same RCA cleaning process. Each of them was deposited with SiN_x only on one side. These polished wafers were used to characterize the optical properties of the layer [thickness and refraction index (RI)] and for Fourier transform infrared spectroscopy (FTIR) measurements to estimate their hydrogen content (see Table I).

Table I: Deposition conditions and layer properties

Layer label	Temperature (°C)	Gas ratio (NH_3/SiH_4)	Pressure (mBar)	Thickness (nm)	RI (at 633 nm)	H fraction as deposit
SiN_x-1	442	2.25	0.17	121.9	2.13	9.92 %
SiN_x-2	442	4.00	0.33	107.7	2.14	10.34 %
SiN_x-3	400	2.25	0.17	120.5	2.14	11.13 %
SiN_x-4	400	4.00	0.33	109.6	2.14	11.36 %
SiN_x-5	350	2.25	0.17	121.8	2.12	12.15 %
SiN_x-6	350	4.00	0.33	113.0	2.12	12.41 %

The six-inch mc-Si wafers were laser cleaved into 3.9 cm × 3.9 cm tokens and underwent firing at six different peak temperatures (589 °C, 645 °C, 676 °C, 748 °C, 798 °C and 858 °C - actual temperature measured on wafer). Subsequently, the wafers were degraded using a laser at 938 nm with an intensity of 46 kW/m^2 and a sample temperature of 140 °C, following the laser-accelerated process proposed by Payne *et al*. [3]. This process was applied for different time-steps, starting with a short time (2 s) in progressive steps until partial lifetime recovery was reached (600 s), allowing for clear identification of any differences in the time dependence of CID at the most degraded point for each wafer. At this stage, the Cz wafers were fired at 748 °C and 795 °C, and the change in the hydrogen fraction of the films was measured using FTIR.

After each laser treatment step, the changes in the effective lifetime of the sample were measured using a photoconductance (PC) lifetime tester (WTC-120, Sinton instruments) along with photoluminescence (PL) imaging (BTI LIS-R1).

3 RESULTS AND DISCUSSION

3.1 *Degradation differences between the different SiN_x layers*:

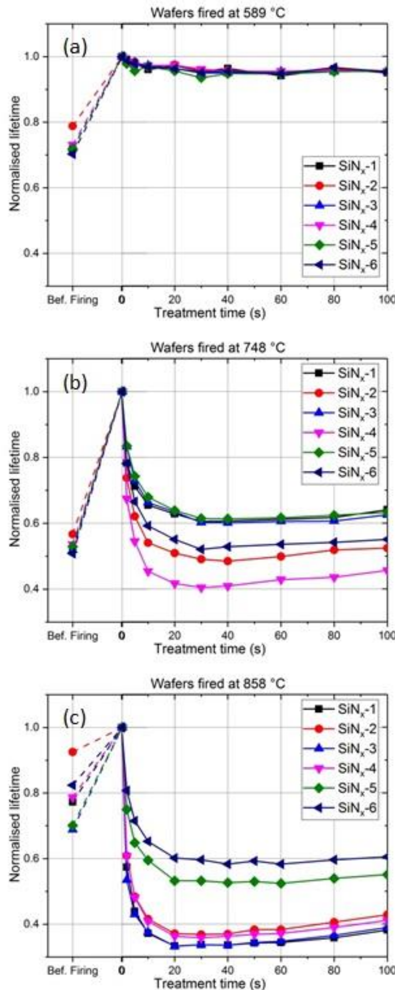

Figure 1: Normalised effective lifetime as a function of the laser treatment time for different SiN_x layers fired at: (a) 589 °C, (b) 748 °C and (c) 858 °C. The firing point corresponds to the zero point in degradation time.

Despite using samples from neighbouring wafers, variations within 10% of the effective lifetime were found between samples before firing; after firing these differences were within 15%, depending on the firing peak temperature [6]. Therefore, in order to identify the changes in the lifetime during the degradation process, independently of the sample effective lifetime after firing (τ_{fire}), the normalised lifetime ($\tau_{norm} = \tau(t) / \tau_{fire}$, where $\tau(t)$ is the effective lifetime after each laser treatment step, including the value before firing) was used. The effective lifetimes were taken at an excess carrier density Δn = $1{\times}10^{15}$ cm^{-3}.

Figures 1 (a)-(c) presents τ_{norm} of the tokens fired at peak temperatures of 589 °C, 748 °C and 858 °C as a function of laser illumination time. At low firing temperature [see Figure 1 (a)], the degradation was weak and slow, as expected [6], and no differences in the CID extent between the different SiN_x layers could be observed. Higher firing temperatures increased the degradation effect [see Figures 1 (b) and (c)] and differences in degradation characteristics between the different SiN_x layers become apparent.

Figures 2 (a) to (d) present PL images of two samples (passivated with SiN_x-1 and SiN_x-4 layers) fired at the same temperature of 748 °C, after firing and in the most degraded state. It is possible to observe how these neighbouring samples degraded differently due to the different SiN_x layers.

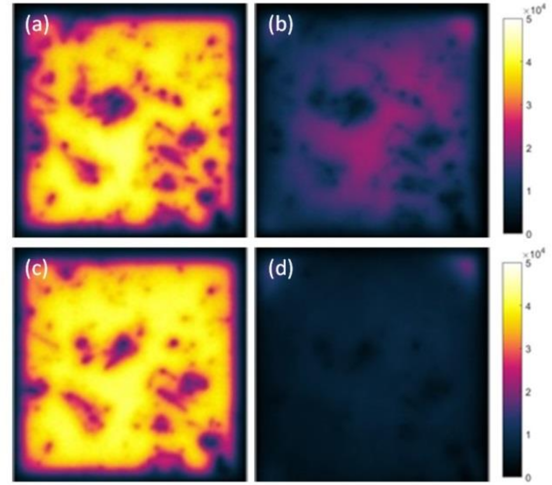

Figure 2: PL images of 3.9 cm × 3.9 cm tokens using 0.3 s of integration time: (a) SiN_x-1 after firing, (b) SiN_x-1 after 30 s of laser treatment, (c) SiN_x-4 after firing, and (d) SiN_x-4 after 30 s of laser degradation.

Figure 3 presents the relative change in the effective lifetime [defined as $(\tau_{deg}-\tau_{fire})/\tau_{fire}{\times}100\%$, where τ_{deg} is the effective lifetime in the most degraded state] due to the degradation. At low firing temperatures (< 650 °C) the degradation is similar for all the samples, independently of the SiN_x layer. However, at higher firing temperatures, a significant difference can be noticed between the different layers. This difference is relevant as most screen-printing pastes require peak firing temperatures of around 800 °C. Similar results were found for other wafer sets and for other firing conditions (not shown here; they will be presented in a future publication).

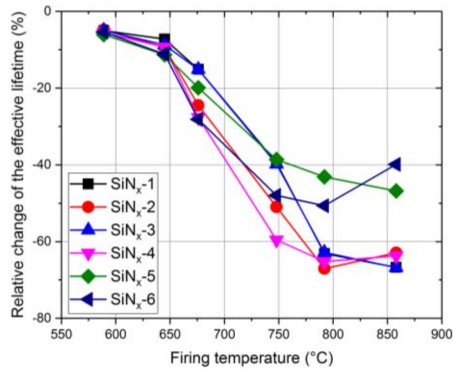

Figure 3: Relative lifetime change due to CID for different firing temperatures and SiN_x passivation layers.

3.2 *Impact of the deposition conditions and hydrogen released during the firing on CID*:

To estimate the amount of hydrogen released from the dielectric layer during firing, we compared the hydrogen content in the films before and after firing. Despite the fact that only a fraction of the released hydrogen would diffuse. Despite the fact that only a fraction of the released hydrogen would diffuse into the bulk, we can infer that greater hydrogen release would correlate to a greater amount of hydrogen penetrating into the wafer. Figure 4 presents the CID extent (defined as the absolute value of the relative change in the effective lifetime) as a function of the fraction of hydrogen released during the firing. The degradation was more pronounced for wafers with SiN_x layers that released a higher hydrogen fraction. Similar results were obtained for other firing temperatures.

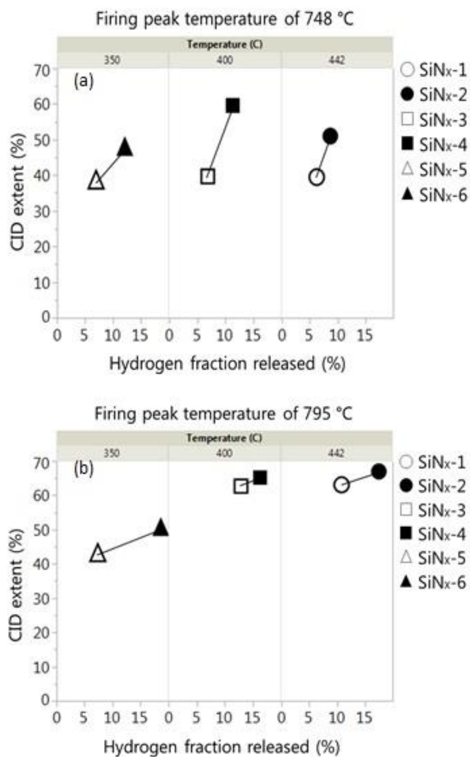

Figure 4: Comparison between the lifetime changes for the wafers fired at 748 °C (a) and 798 °C (b) in terms of the hydrogen fraction released in the firing step and the temperature and pressure of the passivation layer deposition.

This is a first indication that CID may be related to the amount of hydrogen released during the firing step. This indication supports Chan *et al*. [9] and Jensen *et al.* [10] recent suggestion that hydrogen has a role in the formation and passivation of the CID defect. The secondary dependence of the CID extent with the deposition temperature of the SiN_x could be associated with different layer density [8] or differences in the thermal history of the samples [9].

3.3 *Surface recombination changes due to CID*:

Figures 5 (a) and (b) plots the surface recombination saturation current (*Jos*) and the high-injection bulk lifetime (τ_{bulk}; using the Kane and Swanson method [11] as implemented in the Sinton Instruments lifetime tester) extracted at $\Delta n = 2\times10^{16}$ cm^{-3}, before and after the degradation for the tokens fired at 748 °C. No significant change of the surface passivation quality can be noticed (in some cases an improvement can be observed), whilst τ_{bulk} changes considerably. Similar results were found for the wafers fired at other peak temperatures. Therefore, it can be concluded that CID is not associated with changes in the surface recombination and is most likely related to a bulk-defect.

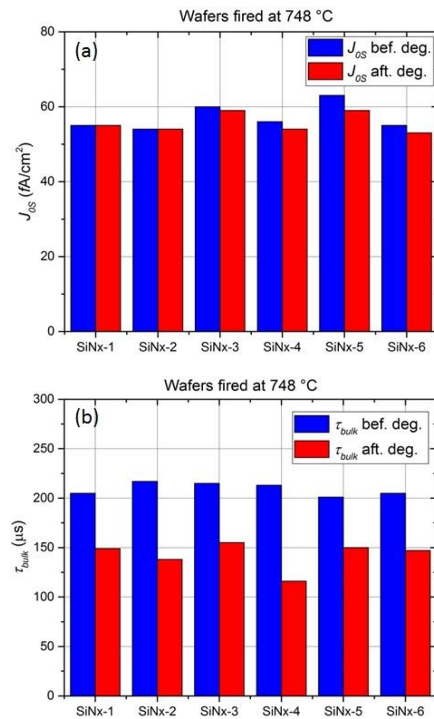

Figure 5: Comparison between the changes in the surface saturation current density (a) and the high-injection bulk lifetime (b) before and after the degradation of wafers fired at 748 °C.

4 CONCLUSIONS

In this contribution, we demonstrated that the SiN_x deposition conditions influence the extent of CID when high firing temperatures are used. A correlation between the hydrogen released during the firing and the degradation was found, indicating a possible link between them. Moreover, we do not detect significant changes in the surface recombination and therefore we concluded that the CID effect is primarily associated with a bulk defect.

REFERENCES

[1] K. Ramspeck *et al.*, “Light induced degradation of rear passivated mc-Si solar cells,” *27th Eur. Photovolt. Sol. Energy Conf. Exhib.*, pp. 861–865, Oct. 2012.

[2] F. Kersten *et al.*, “Degradation of multicrystalline silicon solar cells and modules after illumination at elevated temperature,” *Sol. Energy Mater. Sol. Cells*, vol. 142, pp. 83–86, Nov. 2015.

[3] D. N. R. Payne *et al.*, “Acceleration and mitigation of carrier-induced degradation in *p*-type multi-crystalline silicon,” *Phys Status Solidi–Rapid Res Lett*, vol. 10, no. 3, pp. 237–241, Mar. 2016.

[4] F. Fertig, K. Krauß, and S. Rein, “Light-induced degradation of PECVD aluminium oxide passivated silicon solar cells,” *Phys. Status Solidi - Rapid Res. Lett.*, vol. 9, no. 1, pp. 41–46, Jan. 2015.

[5] F. Kersten, J. Heitmann, and J. W. Müller, “Influence of Al_2O_3 and SiN_x Passivation Layers on LeTID,” *Energy Procedia*, vol. 92, pp. 828–832, Aug. 2016.

[6] C. E. Chan *et al.*, “Rapid stabilization of high-performance multicrystalline *p*-type silicon PERC cells,” *IEEE J. Photovolt.*, vol. 6, no. 6, pp. 1473–1479, Nov. 2016.

[7] D. Bredemeier, D. Walter, S. Herlufsen, and J. Schmidt, “Lifetime degradation and regeneration in multicrystalline silicon under illumination at elevated temperature,” *AIP Adv.*, vol. 6, no. 3, p. 035119, Mar. 2016.

[8] Z. Hameiri, N. Borojevic, L. Mai, N. Nandakumar, K. Kim, and S. Winderbaum, “Low-absorbing and thermally stable industrial silicon nitride films with very low surface recombination,” *IEEE J. Photovolt.*, vol. 7, no. 4, pp. 996–1003, Jul. 2017.

[9] C. Chan *et al.*, “Modulation of carrier-induced defect kinetics in multi-crystalline silicon PERC cells through dark annealing,” *Phys Status Solidi–Rapid Res Lett*, vol. 1, no. 2, p. 1600028, Feb. 2017.

[10] M. A. Jensen, A. E. Morishige, J. Hofstetter, D. B. Needleman, and T. Buonassisi, “Evolution of LeTID defects in *p*-type multicrystalline silicon during degradation and regeneration,” *IEEE J. Photovolt.*, vol. 7, no. 4, pp. 980–987, Jul. 2017.

[11] D. Kane and R. Swason, “Measurement of the emitter saturation current by a contactless photoconductivity decay method,” *18th IEEE Photovolt. Spec. Conf.*, vol. 18, pp. 578–583, 1985.